Spectral distortions at Super-Kamiokande

S. Dev[*] and Sanjeev Kumar[†]

Department of Physics, Himachal Pradesh University, Shimla 171005, India
(Received 27 May 2006; revised manuscript received 31 August 2006; published 13 December 2006)

We examine the effect of the rise in the survival probability of the electron neutrinos with the decrease in the neutrino energy on the recoil electron spectrum at Super-Kamiokande.

The neutral current (NC) measurements at SNO [1] have, conclusively, established the oscillations of the solar neutrinos and after the evidence for terrestrial antineutrino disappearance in a beam of electronic antineutrinos reported by KamLAND [2], all other solutions [3–5] of SNP can, at best, be just subdominant effects. The solar neutrino experiments have, already, entered a phase of precision measurements for oscillation parameters. The completeness of the LMA solution is being questioned [6] and the scope for some possible subdominant transitions is being explored vigorously [7–11]. The presence of these ''new physics'' (NP) effects even at a subdominant level will affect the present determination of the oscillation parameters [11]. As of now, the exact profile of the survival probability of electronic neutrinos over the whole energy spectrum remains unknown as a result of which it is not possible to pin point the exact mechanism(s) of neutrino flavor conversion or to exclude the coexistence of the other subdominant transitions driven by non- standard neutrino-matter interactions/properties. The situation is complicated by the fact that the transition probability in some of these nonstandard NP scenarios [12] is energy-independent implying an undistorted solar neutrino spectrum which is consistent with the Super-Kamiokande and SNO spectral data.

In order to study the effect of the rise in the electron survival probability on the recoil electron spectrum, we define a quantity $S(T)$ as

$$S(T) = \frac{\langle \frac{d\sigma}{dT} \rangle_{\text{LMA}}}{\langle \frac{d\sigma}{dT} \rangle_{\text{SSM}}}$$

$$= \frac{\int_{E_{\min}}^{E_{\max}} dE f(E)[\frac{d\sigma_e}{dT} P(E) + \frac{d\sigma_x}{dT}\{1 - P(E)\}]}{\int_{E_{\min}}^{E_{\max}} dE f(E) \frac{d\sigma_e}{dT}}, \quad (1)$$

where $P(E)$ is the LMA survival probability [13] and $f(E)$ is the standard ^{8}B spectrum [14]. The quantity $S(T)$ has the. The quantity $S(T)$ has the interpretation as the probability of an electron being scattered with a recoil kinetic energy T and closely resembles the SK data/SSM ratio with the only difference that the SK data/SSM ratio is presented for individual energy bins while $S(T)$ as defined above is a

continuous function of recoil electron energy. The tree level cross-sections for $\nu_e e$ and $\nu_x e$ ($x = \mu, \tau$) scattering have been given in Ref. [15]. In fact, $S(T)$ is the LMA expectation for the recoil electron spectrum normalized to the standard ^{8}B neutrino spectrum and has been plotted as a function of T in Fig. 1 along with the $S(T)$ for energy-independent asymptotic value of the LMA survival probability for comparison. The two probabilities differ considerably from each other and this difference could be as large as 10% at 5 MeV. This is enough to highlight the role of spectral distortions in discriminating the LMA suppression scenario from the energy-independent suppression NP scenarios mentioned above [12]. At the current level of precision, both the LMA suppression and the energy-independent suppression are consistent with the SK as well as SNO solar neutrino data. Consequently, one can not claim a conclusive confirmation of the LMA solution from the exclusive study of the high energy region of the solar neutrino spectrum. It is, therefore, imperative to study quantitatively the spectral distortions not only to finally confirm the LMA solution but also to disentangle the possible NP effects.

The probability that a recoil electron with true kinetic energy T_{true} will be detected with the observed kinetic energy T_{obs} is given by

$$r(T_{\text{true}}, T_{\text{obs}}) = \frac{1}{\sqrt{2\pi}\sigma_T} \exp\left(-\frac{(T_{\text{true}} - T_{\text{obs}})^2}{2\sigma_T^2}\right) \quad (2)$$

and is called the detector response function. The energy-dependent spread, σ_T, is of the form
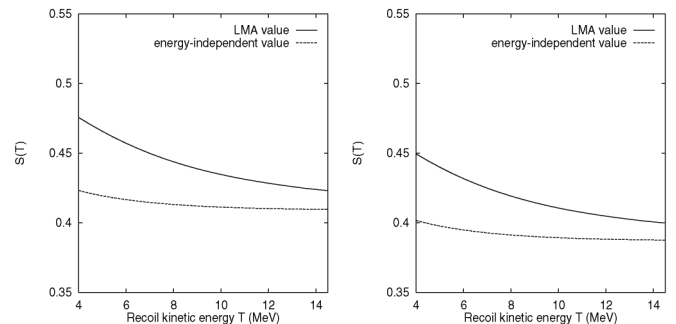

FIG. 1. $S(T)$ versus T for $\theta_{13} = 0°$ (left panel) and $\theta_{13} = 12.3°$ (right panel).

---

[*]Electronic address: dev5703@yahoo.com
[†]Electronic address: sanjeev3kumar@yahoo.co.in

117301-1

$$\sigma_T = \epsilon \sqrt{\frac{T_{\text{true}}}{10 \text{ MeV}}} \tag{3}$$

so that ϵ is the energy spread at 10 MeV. For SK, $\epsilon = 1.4$. To account for the finite energy resolution, the differential cross-section must be folded with the detector response

function, i.e. we must have

$$\left\langle \frac{d\sigma}{dT} \right\rangle (T_{\text{obs}}) = \int_0^\infty dT_{\text{true}} \left\langle \frac{d\sigma}{dT} \right\rangle (T_{\text{true}}) r(T_{\text{true}}, T_{\text{obs}}) \tag{4}$$

in Eq. (1) for $S(T)$ to obtain the observed value of

$$S(T_{\text{obs}}) = \frac{\int_0^\infty dT_{\text{true}} r(T_{\text{true}}, T_{\text{obs}}) \int_{E_{\min}}^{E_{\max}} dE f(E) [\frac{d\sigma_e}{dT_{\text{true}}} P(E) + \frac{d\sigma_x}{dT_{\text{true}}} \{1 - P(E)\}]}{\int_0^\infty dT_{\text{true}} r(T_{\text{true}}, T_{\text{obs}}) \int_{E_{\min}}^{E_{\max}} dE f(E) \frac{d\sigma_e}{dT_{\text{true}}}}. \tag{5}$$

The quantity $S(T_{\text{obs}})$ has been plotted as a function of T_{obs} in Fig. 2 for the LMA value of survival probability as well as the energy-independent asymptotic value (EIAV) of the survival probability. Also shown are the same two curves depicted in Fig. 1 assuming perfect energy resolution. We integrate $S(T_{\text{obs}})$ over the total recoil electron energy $E_{\text{obs}} = T_{\text{obs}} + m_e$ in the bins of 0.5 MeV. This integrated normalized spectrum is denoted by S and has been plotted in Fig. 3 alongwith the actual 1496 d SK spectrum normalized to BP04 with statistical errors only [16]. One can calculate the rise in the LMA value $S_{\text{LMA}}(T_{\text{obs}})$ relative to the energy-independent asymptotic value $S_{\text{EIAV}}(T_{\text{obs}})$ at a particular value of T_{obs} by defining

$$R(T_{\text{obs}}) = \frac{S_{\text{LMA}}(T_{\text{obs}}) - S_{\text{EIAV}}(T_{\text{obs}})}{S_{\text{EIAV}}(T_{\text{obs}})}. \tag{6}$$

It is instructive to see the variation in $R(T_{\text{obs}})$ because of the energy spread ϵ. Figure 4 shows $R(T_{\text{obs}})$ for $\epsilon = 0$ (perfect energy resolution) and for $\epsilon = 1.4$ (finite energy resolution). It is clear that as a result of finite energy resolution of the detector, $S_{\text{LMA}}(T_{\text{obs}})$ and, therefore, $R(T_{\text{obs}})$ gets enhanced as compared to the corresponding values for perfect energy resolution and, again, this increase is more pronounced at the higher energies. Although, the curve for

$R(T_{\text{obs}})$ becomes flatter because of the finite energy resolution of the detector but the actual value of $R(T_{\text{obs}})$ becomes larger which is an advantage. One can compare the value of S in a low energy bin viz. S_L with that in a high energy bin viz. S_H and find the relative increase in S by defining the relative rise-up R as

$$R = \frac{S_L - S_H}{S_H}. \tag{7}$$

It is important to note that R defined above is essentially independent of the flux normalization. Otherwise, it would have been difficult to directly compare S with the experimental data which has to be normalized to the SSM ^{8}B flux which is not known accurately enough. Also, the above definition is, almost, independent of θ_{13} since the factor of $\cos^4\theta_{13}$ cancels in the ratio. A nonzero θ_{13} will suppress $S(T)$ by the factor of $\cos^4\theta_{13}$ but the 'rise-up' R will remain practically unchanged (see Fig. 1). Thus, if the SK spectrum is found to differ from the LMA spectrum, this conflict cannot be reconciled even in a 3-flavor framework since the LMA value of R is the same in two/three-flavor framework for small θ_{13}. This is contrary to some assertions made recently [17] in literature. Moreover, some
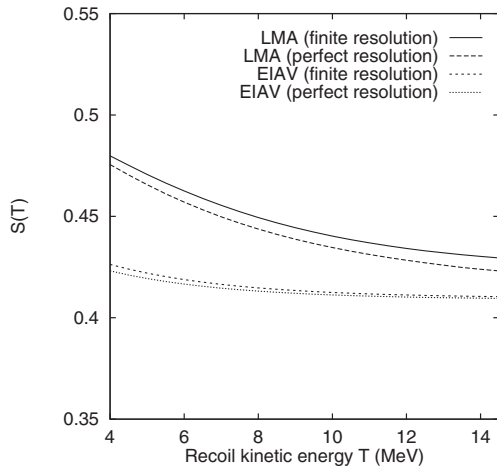
FIG. 2. Probability folded with detector response function and neutrino cross-sections as the function of recoil electron kinetic energy.
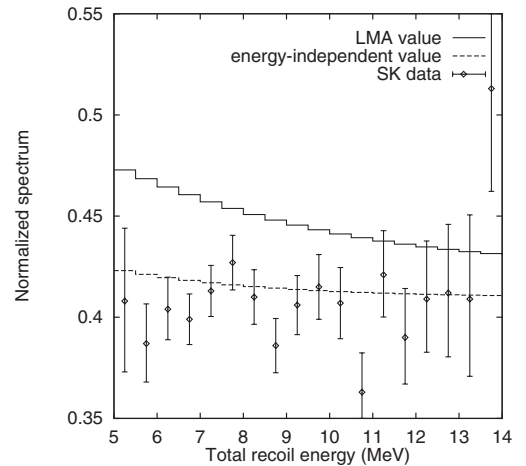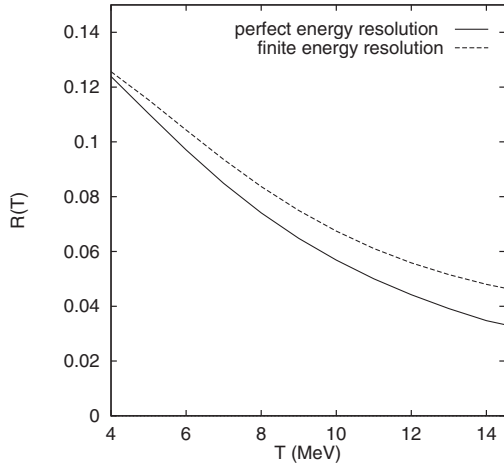
FIG. 3. The recoil electron spectrum normalized to SSM in the bins of 0.5 MeV (S). The SK data with statistical errors is also shown for comparison.

FIG. 4. $R(E_{\mathrm{obs}})$ versus E_{obs}.

FIG. 5.   The rise-up $\mathcal{R}$ in the total (day + night) SSM normalized rate versus θ_{12} for the central and 1σ upper/lower values of Δm^2. The solar mixing angle θ_{12} has been varied over its 1σ range.

part of the energy correlated systematic uncertainties will cancel in $\mathcal{R}$.

The variable $\mathcal{R}$ defined in Eq. (7) can be used as an observable to quantify the turn-up in the data/SSM ratio at SK at low energies. It is different from the global observables like the moments defined in Ref. [18] in the sense that it directly compares the normalized spectral data at two energy ends of the spectrum while the moments are global quantities which are not suitable for this purpose. Moreover, the SK solar neutrino data is, already, available in small energy bins. For the sake of illustration, we choose the bins $E = 5.5$–6.0 MeV and $E = 13.0$–13.5 MeV and evaluate $\mathcal{R}$ for these bins to obtain

$$\mathcal{R} = -0.054 \pm 0.126 \qquad (8)$$

where both the systematic and statistical errors have been incorporated in the analysis. The rise-up is not significantly different from zero for these energy bins. The upper bound on $\mathcal{R}$ is approximately 0.07 (0.20) at 1σ (2σ) C.L.. This is to be compared with the corresponding LMA value of rise-up

$$\mathcal{R}^{\mathrm{day}}_{\mathrm{LMA}} = 0.087^{+0.026}_{-0.016} \qquad (9)$$

for $\Delta m^2 = 7.9 \pm 0.3 \times 10^{-5}$ eV^2 and $\sin^2\theta_{12} = 0.3^{+0.02}_{-0.03}$ where the earth regeneration effects have been neglected. However, the earth regeneration effects can be incorporated in a straight forward manner which yields

$$\mathcal{R}^{\mathrm{night}}_{\mathrm{LMA}} = 0.070^{+0.024}_{-0.015}. \qquad (10)$$

The rise-up in the total (day + night) SSM normalized rate is

$$\mathcal{R}_{\mathrm{LMA}} = 0.078^{+0.025}_{-0.016}. \qquad (11)$$

This LMA value is compatible with the present experimental value [Eq. (8)] within 1σ C.L.. The 'rise-up' $\mathcal{R}$ in the total (day + night) SSM normalized rate has been plotted in Fig. 5 as a function of θ_{12} for the central and 1σ upper/
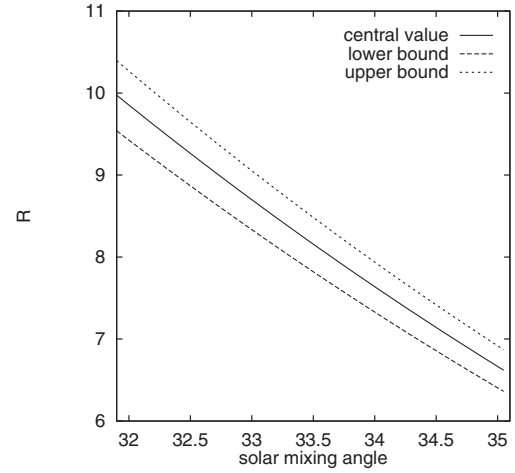
lower values of Δm^2_{12}. Since, the rise-up $\mathcal{R}$ becomes larger for smaller values of θ_{12}, an upper bound on $\mathcal{R}$ can be used to obtain a lower bound on θ_{12} [9]. Figure 6 depicts the improvement in the upper bound on $\mathcal{R}$ with increase in statistics and reduction in systematic errors at Super-Kamiokande. The confidence levels for the measurement of $\mathcal{R}$ with the increase in statistics and a projected reduction in systematic errors at SK have been given in Fig. 7 from which it is clear that with the present level of accuracy at Super-Kamiokande, a rise-up of 20% can be measured at 1.1σ C.L. Not much improvement results even with the increased statistics with the present level of systematic errors. The contribution of *hep* neutrinos for the bins we have examined is very small (about 1.2%) for the SSM value of this flux. However, arbitrarily large values of *hep* flux can substantially affect the higher energy bins with energy greater than 14 MeV.

The enhancement in $S(T)$ for smaller values of T can be used to further constrain the currently allowed neutrino parameter space. We illustrate this point by plotting the
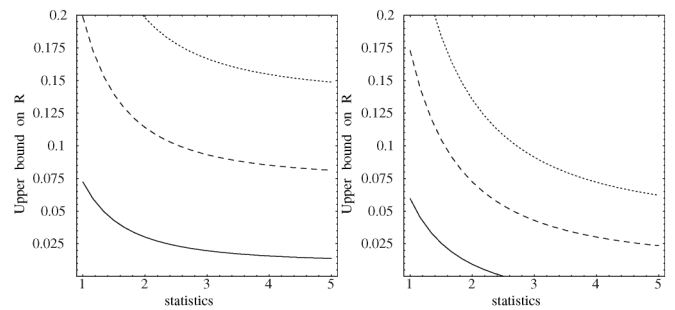

FIG. 6.   Improvements in the upper bound on $\mathcal{R}$ with increased statistics with present (left panel) and half of the present (right panel) systematic errors. The solid, dashed and dotted lines are the upper bounds at 1, 2 and 3σ C.L.
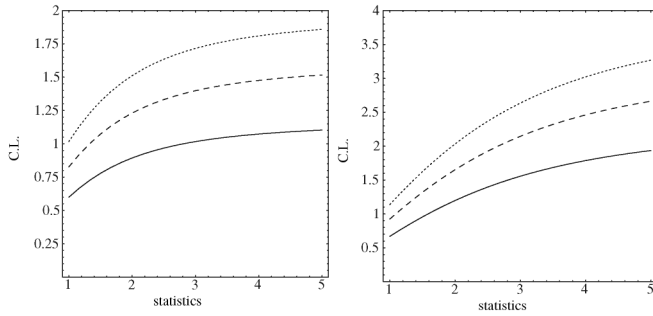
FIG. 7. (a) Confidence levels for the measurement of $\mathcal{R}$ with increase in statistics for present systematic errors (left panel). (b) Confidence levels for the measurement of $\mathcal{R}$ with increase in statistics for half of the present systematic errors (right panel). The solid, dashed and dotted lines are for $\mathcal{R} = 0.10, 0.15$ and 0.20.

FIG. 8. Constant $\mathcal{S}$ and $\mathcal{R}$ plots.

constant $\mathcal{S}$ and $\mathcal{R}$ curves on the $(\Delta m_{12}^2, \theta_{12})$ plane. The quantity $\mathcal{S}$ is obtained by integrating $S(T)$ over the energy bin of 0.5 MeV centered around $T = 5$ MeV and the quantity $\mathcal{R}$ is calculated from Eq. (7) for the energy bins of 0.5 MeV centered around $T = 5$ MeV, 15 MeV. We choose these values for illustrative purposes only. The constant $\mathcal{S}$ and $\mathcal{R}$ curves on the $(\Delta m_{12}^2, \theta_{12})$ plane are shown in Fig. 8 for the $(\Delta m_{12}^2, \theta_{12})$ parameter space within the currently allowed LMA region. For Δm_{12}^2 and θ_{12}, we select the 2σ ranges of these quantities and plot the constant $\mathcal{S}$ curves for $\mathcal{S} = 0.44, 0.46, 0.48$ (curves with negative slope from left to right, respectively) and, also, plot the constant $\mathcal{R}$ curves for $\mathcal{R} = 0.12, 0.10, 0.08$ (curves with positive slope from left to right, respectively). It is evident that there is an increase in $\mathcal{S}$ and decrease in $\mathcal{R}$ with
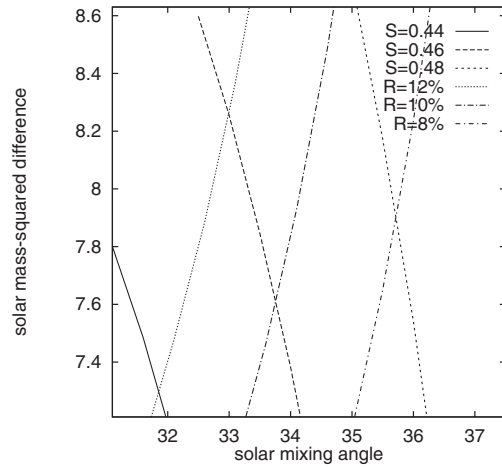
increasing θ_{12}. Therefore, an accurate measurement of $\mathcal{S}$ and $\mathcal{R}$ at 5 MeV will further constrain the LMA allowed θ_{12}. For instance, if $\mathcal{S}$ is found to be smaller than 0.46 (i.e. $\mathcal{S} \leq 0.46$) and $\mathcal{R}$ is found to be less than 12% (i.e. $\mathcal{R} \leq$ 12%), θ_{12} will, approximately, be within the range $31° \leq \theta_{12} \leq 34°$. In conclusion, the prospects for the observation of spectral distortions at SK-III, in case it comes up, appear to be bright [19]. The failure to observe spectral distortions at SK-III would signal new physics beyond LMA.

[1] B. Aharmin *et al.* (SNO Collab.), Phys. Rev. C **72**, 055502 (2005).
[2] K. Eguchi *et al.* (KamLAND Collab.), Phys. Rev. Lett. **90**, 021802 (2003).
[3] C. S. Lim and W. J. Marciano, Phys. Rev. D **37**, 1368 (1988).
[4] B. C. Chauhan, S. Dev, and U. C. Pandey, Phys. Rev. D **59**, 083002 (1999).
[5] E. Kh. Akhmedov and J. Pulido, Phys. Lett. B **485**, 178 (2000); **553**, 7 (2003).
[6] A. Yu. Smirnov, hep-ph/0305106 v2.
[7] P. C. de Holanda and A. Yu. Smirnov, Phys. Rev. D **69**, 113002 (2004).
[8] Bhag C. Chauhan and João Pulido, J. High Energy Phys. 06 (2004) 008.
[9] S. Dev and Sanjeev Kumar, Mod. Phys. Lett. A **20**, 2083 (2005).
[10] S. Dev and Sanjeev Kumar, Mod. Phys. Lett. A **20**, 2957 (2005).
[11] H. Back *et al.*, hep-ex/0412016 and references therein.
[12] J. W. F. Valle, Prog. Part. Nucl. Phys. **26**, 91 (1991); Phys. Lett. B **199**, 432 (1987).
[13] S. J. Parke, Phys. Rev. Lett. **57**, 1275 (1986).
[14] J. N. Bahcall, Nucl. Phys. B, Proc. Suppl. **118**, 77 (2003).
[15] G. t'Hooft, Phys. Lett. B **37**, 195 (1971).
[16] J. Hosaka *et al.* (Super-Kamiokande Collab.), Phys. Rev. D **73**, 112001 (2006).
[17] Bipin Singh Koranga, Mohan Narayan, and S. Uma Sankar, Phys. Rev. D **71**, 095010 (2005).
[18] J. N. Bahcall, P. I. Krastev, and E. Lisi, Phys. Rev. C **55**, 494 (1997).
[19] K. Ishihara (Super-Kamiokande Collab.), ICHEP Report No. ICHEP04, 2004 (unpublished).